

Analytic bond-order potential expansion of recursion-based methods

Bernhard Seiser,¹ D. G. Pettifor,² and Ralf Drautz¹¹ICAMS, Ruhr-Universität Bochum, 44780 Bochum, Germany²Department of Materials, University of Oxford, Parks Road, Oxford OX1 3PH, United Kingdom

(Received 10 December 2012; published 8 March 2013)

We show that the analytic bond-order potentials (BOPs) may be used to reproduce the density of states and energy of recursion-based methods for close-packed atomic configurations. In this way, we demonstrate that the analytic BOPs can efficiently recast the numerical bond-order potentials in a polynomial approximation. By introducing damping factors for the expansion coefficients in analogy to the kernel polynomial method, negative regions of the density of states are removed such that the analytic BOPs may be applied also to open systems with band gaps. By estimating higher moments from the termination of the Lanczos recursion chain, we, furthermore, achieve a faster convergence than the usual kernel polynomial method at a negligible additional computational cost.

DOI: [10.1103/PhysRevB.87.094105](https://doi.org/10.1103/PhysRevB.87.094105)

PACS number(s): 71.15.Nc, 71.20.Be, 61.50.Lt

I. INTRODUCTION

A local evaluation of the energy in electronic structure calculations that has inherently linear scaling may be achieved by reconstructing the local density of states $n_{i\alpha}(E)$ of orbital α on atom i from its moments. The moments of the local density of states $n_{i\alpha}(E)$ may be evaluated from the positions and types of atoms in the vicinity of atom i . In particular, for an orthonormal basis, the n th moment of the local density of states may be obtained by computing all self-returning hopping paths that include $n - 1$ multiplications of the Hamiltonian matrix,¹

$$\begin{aligned}\mu_{i\alpha}^{(n)} &= \int E^n n_{i\alpha}(E) dE = \langle i\alpha | \hat{H}^n | i\alpha \rangle \\ &= \sum_{i_1\alpha_1, i_2\alpha_2, \dots, i_{n-1}\alpha_{n-1}} \langle i\alpha | \hat{H} | i_1\alpha_1 \rangle \langle i_1\alpha_1 | \hat{H} | i_2\alpha_2 \rangle \\ &\quad \dots \langle i_{n-1}\alpha_{n-1} | \hat{H} | i\alpha \rangle,\end{aligned}\quad (1)$$

where the Hamiltonian matrix elements are given by $H_{i\alpha j\beta} = \langle i\alpha | \hat{H} | j\beta \rangle$ for orbitals α and β on atoms i and j , respectively. Therefore the calculation of the moments of the density of states is reduced to a series of matrix multiplications.

In a practical calculation, the evaluation of the moments is the computationally most expensive part. The reconstruction of the density of states and the energy should therefore converge as quickly as possible as a function of the number of moments. It is well known that a minimum of four moments are sufficient to recover structural trends from open to close-packed and to discriminate fcc from bcc, while six moments are required to resolve the energy difference between hcp and fcc.^{2–5} At nine moments, one generally can obtain a good agreement with tight-binding reference calculations, although some structures require 12 or more moments for the resolution of the very small structural energy differences,⁶ while elastic constants may require up to 20 or 30 moments before they converge to the tight-binding reference value.⁷

A number of different methods for approximating the density of states and the binding energy from moments, or equivalently from recursion coefficients, have been developed.^{8–10} In the recursion-based methods, the density of states is approximated by a continued fraction.^{11,12} The numerical bond-order potentials extend the recursion method and provide

efficient forces that converge to the exact gradients of the energy as a function of the number of moments.^{13–16} The kernel-polynomial method (KPM) obtains an expansion of the density of states from the moments in terms of Chebyshev polynomials of the first kind;^{17,18} the Fermi operator expansion (FOE)^{19,20} is based on the expansion of a step function in terms of Chebyshev polynomials of the first kind and may be related to the KPM.²¹ The analytic atom-based bond-order potentials (BOPs) were derived as a systematic extension of the Finnis-Sinclair potential²² from a moments-based perturbation expansion of the continued fraction approximation in terms of Chebyshev polynomials of the second kind and include exact forces for a locally varying bandwidth.^{14,23,24}

In Sec. II of this paper, we will briefly review the analytic BOPs, discuss the expansion of the density of states in terms of the Chebyshev polynomials of the second kind and how this expansion may be written in terms of Chebyshev polynomials of the first kind. We then cast the continued fraction representation of the density of states of the recursion method in the form of the analytic bond-order potentials in Sec. III. In contrast to the numerical bond-order potentials, the expressions for the forces remain the exact negative gradients of the energy at any level of approximation. In Sec. IV, we summarize how the KPM avoids spurious negative densities of states, show how this may be adapted to the analytic BOPs, and illustrate the performance of the resulting analytic BOPs for silicon. After a short summary on the forces for the analytic BOPs in Sec. V, we conclude in Sec. VI.

II. ANALYTIC BOND-ORDER POTENTIALS

The analytic BOPs provide an approximate representation of the tight-binding energy including analytic Hellmann-Feynman-type forces that correspond to exact gradients of the energy.^{23,24} This representation of the tight-binding approximation is achieved by expanding the local density of states $n_{i\alpha}(\varepsilon)$ as a linear combination of Chebyshev polynomials of the second kind:

$$n_{i\alpha}^{(n_{\max})}(\varepsilon) = \frac{2}{\pi} \sqrt{1 - \varepsilon^2} \left[1 + \sum_{n=1}^{n_{\max}} \sigma_{i\alpha}^{(n)} U_n(\varepsilon) \right], \quad (2)$$

where the energy E for the density of states of an atomic orbital $i\alpha$ has been shifted to be centered on $a_{i\alpha}^{(\infty)}$ and normalized by half the bandwidth $W = 4b_{i\alpha}^{(\infty)}$,

$$\varepsilon = \frac{E - a_{i\alpha}^{(\infty)}}{2b_{i\alpha}^{(\infty)}}, \quad (3)$$

such that the density of states is contained in $-1 \leq \varepsilon \leq 1$. The values of $a_{i\alpha}^{(\infty)}$ and $b_{i\alpha}^{(\infty)}$ have to be estimated and must be chosen in such a way that the true density of states is contained in the interval $-1 \leq \varepsilon \leq 1$. Details on how we estimate the bandwidth are given in Appendix B. The expansion coefficients are given by $\sigma_{i\alpha}^{(n)}$ and $U_n(\varepsilon)$ are Chebyshev polynomials of the second kind. The BOP expansion (2) may be viewed as a perturbation expansion with respect to the semi-infinite constant linear chain. At the lowest level of approximation, $n_{i\alpha}(\varepsilon) \propto \sqrt{1 - \varepsilon^2}$, the DOS is given by a simple square root function, which leads to the well-known $\sqrt{\mu_i^{(2)}}$ behavior of the Finnis-Sinclair potential,²² which is also closely related to the embedded-atom method.²³ The expansion coefficients are given by the Chebyshev moments:

$$\sigma_{i\alpha}^{(n)} = \langle i\alpha | U_n(\hat{h}) | i\alpha \rangle = \int_{-1}^{+1} U_n(\varepsilon) n_{i\alpha}(\varepsilon) d\varepsilon = \sum_{m=0}^n p_{nm} \hat{\mu}_{i\alpha}^{(m)}, \quad (4)$$

with

$$\hat{h} = \frac{\hat{H} - a_{i\alpha}^{(\infty)}}{2b_{i\alpha}^{(\infty)}}, \quad (5)$$

and where p_{nm} are the coefficients of the Chebyshev polynomials of the second kind, $U_n(\varepsilon) = \sum_{m=0}^n p_{nm} \varepsilon^m$, and $\hat{\mu}_{i\alpha}^{(m)}$ are the normalized moments of the local density of states:

$$\begin{aligned} \hat{\mu}_{i\alpha}^{(m)} &= \langle i\alpha | \hat{h}^m | i\alpha \rangle = \int \varepsilon^m n_{i\alpha}(\varepsilon) d\varepsilon \\ &= \frac{1}{(2b_{i\alpha}^{(\infty)})^m} \sum_{n=0}^m \binom{m}{n} (-1)^n (a_{i\alpha}^{(\infty)})^n \mu_{i\alpha}^{(m-n)}. \end{aligned} \quad (6)$$

The representation of the local density of states, Eq. (2), may be integrated analytically such that explicit expressions for the number of electrons and the energy may be obtained.^{23,24} By making use of the identity

$$\sin(n+1)\phi = \sqrt{1 - \varepsilon^2} U_n(\varepsilon), \quad (7)$$

with $\cos \phi = -\varepsilon$, it is clear that the expansion of the density of states in Eq. (2) represents a Fourier series on the interval $[0, \pi]$:

$$n_{i\alpha}^{(n_{\max})}(\varepsilon) = \frac{2}{\pi} \sum_{n=0}^{n_{\max}} \sigma_{i\alpha}^{(n)} \sin(n+1)\phi, \quad (8)$$

with $\sigma_{i\alpha}^{(0)} = 1$.

The KPM^{17,21} or the FOE¹⁹ base their expansions on the Chebyshev polynomials of the first kind, $T_n(\varepsilon)$. The Chebyshev polynomials of the first kind are given by

$$T_n(\varepsilon) = \cos n\phi, \quad (9)$$

such that the expansion of the density of states, Eq. (2), may be rewritten in terms of Chebyshev polynomials of the first

kind by using the identity

$$(1 - \varepsilon^2) U_n(\varepsilon) = \frac{1}{2} [T_{n+2}(\varepsilon) - T_n(\varepsilon)], \quad (10)$$

and therefore

$$\begin{aligned} n_{i\alpha}^{(n_{\max})}(\varepsilon) &= \frac{2}{\pi} \sqrt{1 - \varepsilon^2} \sum_{n=0}^{n_{\max}} \sigma_{i\alpha}^{(n)} U_n(\varepsilon), \\ &= \frac{1}{\pi} \frac{1}{\sqrt{1 - \varepsilon^2}} \left[\tau_{i\alpha}^{(0)} + 2 \sum_{n=1}^{n_{\max}+2} \tau_{i\alpha}^{(n)} T_n(\varepsilon) \right], \end{aligned} \quad (11)$$

where the expansion coefficients $\tau_{i\alpha}^{(n)}$ of the density of states in terms of Chebyshev polynomials of the first kind are given by

$$\tau_{i\alpha}^{(0)} = 1, \quad (12)$$

$$\tau_{i\alpha}^{(n)} = \frac{1}{2} [\sigma_{i\alpha}^{(n)} - \sigma_{i\alpha}^{(n-2)}] \quad \text{for } n > 1, \quad (13)$$

and with $\sigma_{i\alpha}^{(-1)} = \sigma_{i\alpha}^{(n_{\max}+1)} = \sigma_{i\alpha}^{(n_{\max}+2)} = 0$. This demonstrates that for practical applications, we may therefore assume that the expansions of the density of states in first kind or second kind of Chebyshev polynomials are equivalent. Because of the direct relation of the expansion (2) to the Finnis-Sinclair second-moment model, we continue to work with the expansion in terms of Chebyshev polynomials of the second kind, although working with Chebyshev polynomials of the first kind is sometimes more straightforward, which will also become apparent in Sec. IV.

III. RELATION TO THE RECURSION EXPANSION

The recursion expansion for the density of states $n_{i\alpha}(E)$ is computed within an $\mathcal{O}(N)$ approach by using the Lanczos algorithm.^{11,25} The algorithm transforms the original Hamiltonian matrix into the form of a semi-infinite one-dimensional nearest-neighbor chain by applying the recurrence relation

$$b_{n+1}|u_{n+1}\rangle = (\hat{H} - a_n)|u_n\rangle - b_n|u_{n-1}\rangle, \quad (14)$$

with $b_0 = 0$ and $|u_0\rangle = |i\alpha\rangle$, where the only nonvanishing matrix elements are given by

$$\langle u_m | \hat{H} | u_n \rangle = \begin{cases} a_n & \text{if } m = n, \\ b_n & \text{if } m = n - 1, \\ b_{n+1} & \text{if } m = n + 1. \end{cases} \quad (15)$$

Since the resultant Hamiltonian matrix is tridiagonal with respect to the Lanczos orbitals u_n , the diagonal matrix element of the Green's function corresponding to the starting state $G_{00} = \langle u_0 | \hat{G} | u_0 \rangle = \langle u_0 | (E - \hat{H})^{-1} | u_0 \rangle$ may be immediately written as a continued fraction expansion.²⁵

$$G_{00}(E) = \frac{1}{E - a_0 - \frac{b_1^2}{E - a_1 - \frac{b_2^2}{E - a_2 - \frac{b_3^2}{\ddots}}}}. \quad (16)$$

If the starting Lanczos orbital $|u_0\rangle$ is chosen as the atomic orbital $|i\alpha\rangle$, the local density of states is given by

$$n_{i\alpha}(E) = -\frac{1}{\pi} \text{Im} G_{00}(E). \quad (17)$$

The recursion coefficients $\{a_n, b_n\}$ that enter the continued fraction may be expressed in terms of the moments of the density of states:

$$\mu_{i\alpha}^{(1)} = a_0, \quad (18)$$

$$\mu_{i\alpha}^{(2)} = a_0^2 + b_1^2, \quad (19)$$

$$\mu_{i\alpha}^{(3)} = a_0^3 + 2a_0b_1^2 + a_1b_1^2, \quad (20)$$

\vdots

For higher moments, the relation between the moments and the recursion coefficients is best calculated recursively, see Appendix A. The inverse relation, namely, the expression of the recursion coefficients in terms of the moments, may also be obtained iteratively.^{11,26} The first few recursion coefficients are obtained as

$$a_0 = \mu_{i\alpha}^{(1)}, \quad (21)$$

$$b_1 = \sqrt{\mu_{i\alpha}^{(2)} - [\mu_{i\alpha}^{(1)}]^2}, \quad (22)$$

$$a_1 = \frac{\mu_{i\alpha}^{(3)} - [\mu_{i\alpha}^{(1)}]^3}{\mu_{i\alpha}^{(2)} - [\mu_{i\alpha}^{(1)}]^2} - 2\mu_{i\alpha}^{(1)}, \quad (23)$$

\vdots

In a practical calculation, only the first n_{\max} moments or equivalently the first $n_{\text{rec}} = n_{\max}/2$ recursion coefficients $\{a_n, b_n\}$ are calculated explicitly. One then terminates the recursion chain by assuming values for the recursion coefficients for $n > n_{\text{rec}}$.^{27–29} The simplest terminator that is typically used in the numerical bond-order potentials assumes $a_n = a_{i\alpha}^{(\infty)}$ and $b_n = b_{i\alpha}^{(\infty)}$ for $n > n_{\max}$.

Here, we show that the analytic BOPs may be used to approximate the density of states of the numerical BOPs. To this end, the moments of the continued fraction representation of the density of states are calculated from the tridiagonal representation of the Hamiltonian (15). The direct evaluation of the Chebyshev moments $\sigma_{i\alpha}^{(n)} = \langle i\alpha | U_n(\hat{h}) | i\alpha \rangle$ is numerically much more robust than the calculation of the moments and therefore is used in a practical implementation, the required expressions are given in Appendix A. The representation of the density of states then follows Eq. (2), but we separate the n_{\max} expansion coefficients, which were actually calculated directly and, therefore, are exact, from the expansion coefficients up to n_{exp} , which were obtained from the terminator and, therefore, are approximate, by writing

$$n_{i\alpha}^{(n_{\max})}(\varepsilon) = \frac{2}{\pi} \sqrt{1 - \varepsilon^2} \times \left[1 + \sum_{n=1}^{n_{\max}} \sigma_{i\alpha}^{(n)} U_n(\varepsilon) + \sum_{n=n_{\max}+1}^{n_{\text{exp}}} \sigma_{i\alpha}^{(n)} U_n(\varepsilon) \right]. \quad (24)$$

The left-hand column of Fig. 1 shows the density of states of the bcc, fcc, and hcp structures for the continued fraction approximation for $n_{\max} = 9$ and terminator with constant $a_{i\alpha}^{(\infty)}$ and $b_{i\alpha}^{(\infty)}$ together with the BOP expansions using $n_{\text{exp}} = 30$,

50, and 100 moments, respectively, and the tight-binding (TB) reference DOS. The calculations were carried out using the canonical d -band bond integrals $dd\sigma : dd\pi : dd\delta = -6:4:-1$.^{30,31} Only first nearest neighbors were retained for the fcc and ideal hcp structures; for bcc, second nearest neighbors were also included assuming that the bond integrals fall off with distance as the inverse fifth power.³⁰ The values of $a_{i\alpha}^{(\infty)}$ and $b_{i\alpha}^{(\infty)}$ were chosen as discussed in Appendix B.

At $n_{\text{exp}} = 100$ moments, the analytic BOP expansion very closely reproduces the continued fraction at an additional computational expense that corresponds to less than 1% of the CPU time required for the calculation of the nine moments in the continued fraction expansion. In fact, the agreement is so close that in the left-hand column of Fig. 1 the density of states of the continued fraction expansion and the BOP expansion with $n_{\text{exp}} = 50$ and 100, respectively, cannot be discerned. Only the BOP expansion with $n_{\text{exp}} = 30$ shows small differences compared to the continued fraction expansion.

Because the moments of the continued fraction density of states and its analytic approximation agree up to 30, 50, and 100 moments, respectively, from the moments theorem,^{2,3} the analytic BOP expansion must oscillate around the continued fraction density of states. This may immediately be understood by considering that the Chebyshev expansion coefficients of the two DOS are equivalent up to 30, 50, and 100 Chebyshev moments, such that the difference between the two DOS is given to leading order by a Chebyshev polynomial of order 31, 51, and 101, respectively. As illustrated in Fig. 1, for a convergent expansion, the difference in the two densities of states becomes smaller the more moments are taken into account.

The close agreement between the continued fraction and the BOP expansion density of states leads to a very close agreement of the bond energy

$$U_{\text{bond},i} = \sum_{\alpha} \int_{\alpha}^{E_F} (E - E_{i\alpha}) n_{i\alpha}(E) dE, \quad (25)$$

where for the purpose of Fig. 1, α sums over the five d orbitals. In the right-hand column of Fig. 1, the bond energy obtained from the numerical integration of the continued fraction density of states and the analytic bond energy from the BOP expansion agree so well that tiny differences are visible only for $n_{\text{exp}} = 30$, whereas for $n_{\text{exp}} = 50$ or 100 the continued fraction and the analytic BOP expansion are virtually identical.

Obtaining Chebyshev moments from the terminator of the recursion chain may be viewed as a way of estimating higher moments when only few moments are known exactly. Alternatively, higher moments may be estimated, for example, from a stochastic evaluation of the moments or the maximum entropy method.^{21,32–34} We think that computing higher moments from the recursion chain is particularly attractive, however, as the analytic BOP expansion converges smoothly towards the recursion expansion while the resulting potential is still fully analytic so that the exact forces may be obtained by straightforward differentiation.

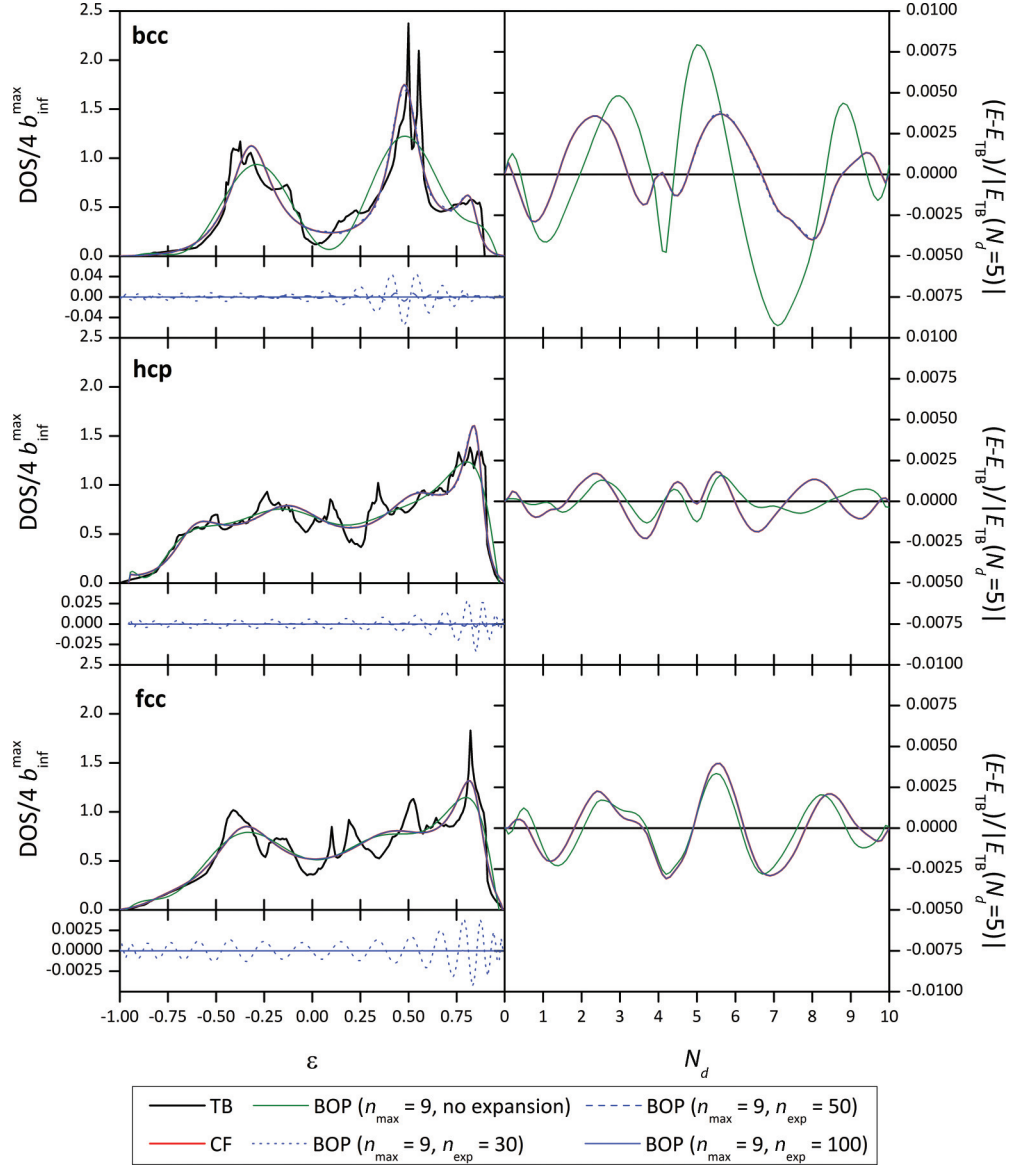


FIG. 1. (Color online) (Left) Comparison of bcc, fcc, and ideal hcp d -band densities of states within the ninth-moment $n_{max} = 9$ expansion. Shown are the tight-binding reference, the continued fraction approximation, and the analytic BOP expansions with $n_{exp} = 30, 50, 100$. Below the DOS, the difference between the continued fraction and the BOP expansion is shown. (Right) Normalized bond energy differences between the tight-binding reference, the continued fraction approximation, and the analytic BOP expansion. Already for $n_{exp} = 30$, the analytic BOPs and continued fraction reference can hardly be differentiated in the plot, while for $n_{exp} = 100$, the difference between continued fraction and analytic BOPs is smaller than the linewidth used in the plot.

IV. EXPLICITLY POSITIVE DENSITY OF STATES

The representation of the density of states of the analytic BOPs in the form of a Fourier series, Eq. (8), makes it apparent that the expansion will, in general, suffer from Gibbs ringing, which may potentially result in a poor and wildly oscillating representation of the density of states. A number of methods exist to remove the Gibbs ringing from a Fourier sum and in the following we will summarize briefly the steps taken in the KPM.^{17,18} One starts by rewriting the expansion (2) of the density of states in the form of an integral equation,

$$n_{i\alpha}^{(n_{max})}(\epsilon) = \int K^{(n_{max})}(\epsilon, \epsilon') n_{i\alpha}(\epsilon') d\epsilon', \quad (26)$$

where $n_{i\alpha}(\epsilon)$ is the true local density of states, and then finds expressions for the kernel $K(\epsilon, \epsilon')$ that make the resultant expansion for $n_{i\alpha}^{(n_{max})}(\epsilon)$ smooth. In KPM, the kernel is expanded in Chebyshev polynomials of the first kind:

$$K^{(n_{max})}(\epsilon, \epsilon') = \frac{1}{\pi} \frac{1}{\sqrt{1 - \epsilon^2}} \left[g_T^{(0)} + 2 \sum_{n=1}^{n_{max}} g_T^{(n)} T_n(\epsilon) T_n(\epsilon') \right]. \quad (27)$$

Inserting this representation of the kernel in Eq. (26) leads to a representation of the density of states:

$$n_{i\alpha}^{(n_{max})}(\epsilon) = \frac{1}{\pi} \frac{1}{\sqrt{1 - \epsilon^2}} \left[g_T^{(0)} \tau_{i\alpha}^{(0)} + 2 \sum_{n=1}^{n_{max}} g_T^{(n)} \tau_{i\alpha}^{(n)} T_n(\epsilon) \right]. \quad (28)$$

If the kernel in Eq. (26) is strictly positive, $K^{(n_{\max})}(\varepsilon, \varepsilon') \geq 0$, then, because the density of states is positive too, $n_{i\alpha}(\varepsilon) \geq 0$, the resulting approximate density of states, in principle, also fulfills $n_{i\alpha}^{(n_{\max})}(\varepsilon) \geq 0$. A positive kernel may be obtained by using the trigonometric form of the Chebyshev polynomials, Eq. (9), such that the kernel is represented as

$$K^{(n_{\max})}(\varepsilon, \varepsilon') = \frac{1}{\pi} \frac{1}{\sin \phi} \left\{ g_T^{(0)} + \sum_{n=1}^{n_{\max}} g_T^{(n)} [\cos n(\phi - \phi') + \cos n(\phi + \phi')] \right\}, \quad (29)$$

where we used $2 \cos \phi \cos \phi' = \cos(\phi - \phi') + \cos(\phi + \phi')$. Therefore, in order to establish the positivity of the kernel, it suffices to show that

$$D(\alpha) = g_T^{(0)} + 2 \sum_{n=1}^{n_{\max}} g_T^{(n)} \cos n\alpha \geq 0, \quad (30)$$

for arbitrary α . Examples of positive kernels are the Fejer kernel,

$$g_T^{(n)} = 1 - \frac{n}{n_{\max}}, \quad (31)$$

and the Jackson kernel that is used in the KPM,²¹

$$g_T^{(n)} = \frac{n_{\max} - n + 1}{n_{\max} + 1} \left(\cos \pi \frac{n}{n_{\max} + 1} + \sin \pi \frac{n}{n_{\max} + 1} \cot \pi \frac{1}{n_{\max} + 1} \right). \quad (32)$$

In practice, a positive kernel does not necessarily mean that the representation of the density of states is positive everywhere, as the band center and band width, $a_{i\alpha}^{(\infty)}$ and $b_{i\alpha}^{(\infty)}$, are parameters that need to be chosen prior to the expansion. If, for example, the bandwidth is chosen too narrow, then the kernel cuts out only part of the true density of states. Therefore the expansion coefficients $\tau_{i\alpha}^{(n)}$ that one would obtain from carrying out the integral over the kernel explicitly no longer agree with the expansion coefficients that are calculated from the moments theorem. Thus, if the expansion coefficients that are obtained based on the moments theorem are entered into Eq. (28), the density of states may become negative although the kernel is positive. Therefore the choice of $a_{i\alpha}^{(\infty)}$ and $b_{i\alpha}^{(\infty)}$ is critical for a sensible expansion of the density of states. Here, we use the Gerschgorin circle theorem³⁵ to guarantee that the band width and band center are chosen in such a way that the complete spectrum $n_{i\alpha}(E)$ is covered and therefore the expansion of the density of states is strictly positive, see Appendix B.

We show how to achieve an explicitly positive representation of the density of states in the analytic bond-order potentials by following the KPM and expanding the kernel in Chebyshev polynomials of the second kind:

$$K^{(n_{\max})}(\varepsilon, \varepsilon') = \frac{2}{\pi} \sqrt{1 - \varepsilon^2} \left[g_U^{(0)} + \sum_{n=1}^{n_{\max}} g_U^{(n)} U_n(\varepsilon) U_n(\varepsilon') \right], \quad (33)$$

such that the density of states may be written in the form of Eq. (2) modified by the kernel expansion coefficients $g_U^{(n)}$,

$$n_{i\alpha}^{(n_{\max})}(\varepsilon) = \frac{2}{\pi} \sqrt{1 - \varepsilon^2} \left[g_U^{(0)} + \sum_{n=1}^{n_{\max}} g_U^{(n)} \sigma_{i\alpha}^{(n)} U_n(\varepsilon) \right]. \quad (34)$$

By using $U_n = \sin(n+1)\phi / \sin \phi$, the representation of the kernel is equivalent to

$$K^{(n_{\max})}(\varepsilon, \varepsilon') = \frac{1}{\pi} \frac{1}{\sin \phi'} \left\{ \sum_{n=1}^{n_{\max}+1} g_U^{(n-1)} [\cos n(\phi - \phi') - \cos n(\phi + \phi')] \right\}, \quad (35)$$

where we used $2 \sin \phi \sin \phi' = \cos(\phi - \phi') - \cos(\phi + \phi')$. By comparing to Eq. (29), we may choose to identify

$$g_U^{(n)} = g_T^{(n+1)} / g_T^{(1)}, \quad n = 1, \dots, n_{\max}, \quad (36)$$

where the coefficients $g_T^{(n+1)}$ are the coefficients of an expansion in terms of Chebyshev polynomials of the first kind that includes terms up to order $n_{\max} + 1$. In Fig. 2, the kernel that is obtained in this way is illustrated.

An explicitly positive kernel may be obtained as follows. As ϕ and ϕ' are limited to the interval $[0, \pi]$ and because of the symmetry of the cosine function, we may rewrite the kernel (33) as

$$K^{(n_{\max})}(\varepsilon, \varepsilon') = \frac{1}{2\pi} \frac{1}{\sin \phi'} \left[\sum_{n=1}^{n_{\max}+1} g_U^{(n-1)} (\cos n\alpha - \cos n\beta) \right], \quad (37)$$

with $\alpha = |\phi - \phi'|$ and $\beta = \pi - |\phi + \phi' - \pi|$, where $0 \leq \alpha \leq \beta \leq \pi$. Therefore the kernel is positive if

$$\sum_{n=1}^{n_{\max}+1} g_U^{(n-1)} \cos n\alpha \geq \sum_{n=1}^{n_{\max}+1} g_U^{(n-1)} \cos n\beta. \quad (38)$$

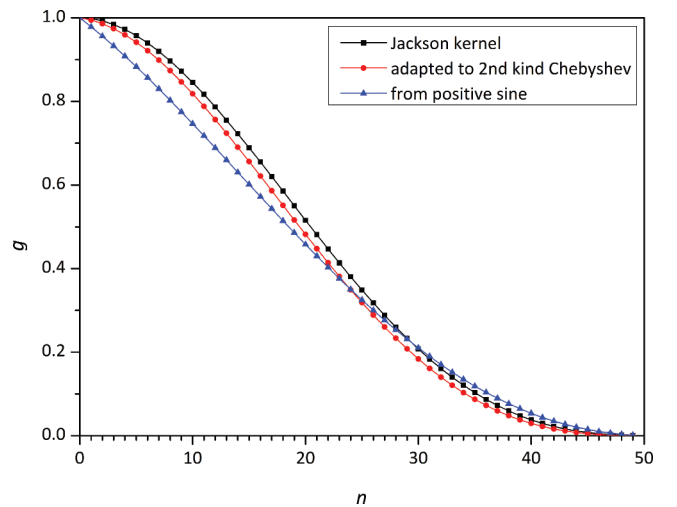


FIG. 2. (Color online) Jackson kernel, Eq. (32), for Chebyshev polynomials of the first kind for $n_{\max} = 50$ (black squares), and the corresponding kernels, Eqs. (36) (red circles) and (40) (blue triangles), for Chebyshev polynomials of the second kind.

As this inequality has to hold for arbitrary $\alpha \leq \beta$, this implies that the sum $\sum_{n=1}^{n_{\max}+1} g_U^{(n-1)} \cos n\alpha$ has to decrease when α is increased and, therefore, Eq. (38) may be fulfilled by a first derivative that is smaller than or equal to zero:

$$\sum_{n=1}^{n_{\max}+1} n g_U^{(n-1)} \sin n\alpha \geq 0. \quad (39)$$

A detailed discussion of positive sine polynomials may be found in Ref. 36. The authors also show that a positive cosine polynomial may be used to generate a positive sine polynomial. Their Eq. (2.13) may be adopted to Eq. (39), from which it follows that a positive kernel expansion using Chebyshev polynomials of the second kind may be obtained directly from a positive kernel expansion using Chebyshev polynomials of the first kind from the simple relation

$$\begin{aligned} g_U^{(n)} &= \kappa \frac{g_T^{(n)} - g_T^{(n+2)}}{n+1}, \quad n = 0, \dots, n_{\max} - 2, \\ g_U^{(n_{\max}-1)} &= \kappa \frac{g_T^{(n_{\max}-1)}}{n_{\max}}, \\ g_U^{(n_{\max})} &= \kappa \frac{g_T^{(n_{\max})}}{n_{\max} + 1}, \end{aligned} \quad (40)$$

with $\kappa = 1/(g_T^{(0)} - g_T^{(2)})$ to ensure $g_U^{(0)} = 1$. The resulting, strictly positive kernel is slightly broader than the kernel obtained from the simple adaption of the Jackson kernel in Eq. (36) but has the advantage that because of Eq. (39), the first derivative is smooth, in addition to the positivity of the kernel, which removes the fast oscillations that are displayed by Eq. (36). In Fig. 2, the two kernels are compared for $n_{\max} = 50$, and in Fig. 3, the convergence of the kernels is illustrated.

Because of the significant damping and reduction of the expansion coefficients $\sigma_{i\alpha}^{(n)}$ for n close to n_{\max} , the kernel polynomial method converges only slowly as a function of the maximum number of moments used in the expansion. For example, the analytic BOP $n_{\max} = 9$ -moments density of

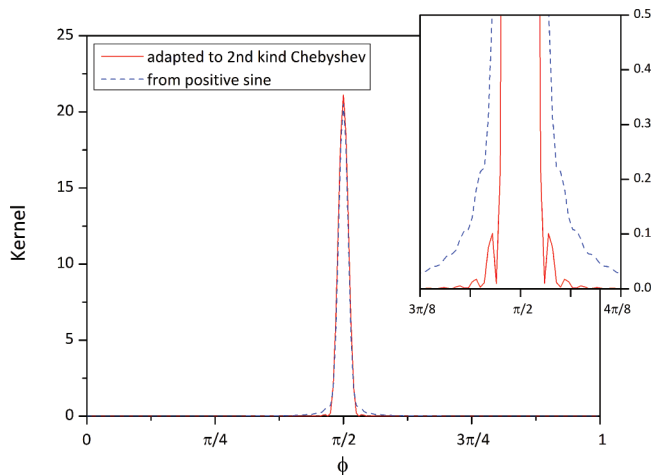


FIG. 3. (Color online) Cut through the kernel $D(\phi, \phi') = \{\sum_{n=1}^{n_{\max}+1} g_U^{(n-1)} [\cos n(\phi - \phi') - \cos n(\phi + \phi')]\}$ for $n_{\max} = 50$ and $\phi' = \pi - \phi$. Equations (36) (red line) and (40) (blue dashed) derived from the Jackson kernel.

states of an fcc crystal shows a reasonable agreement with the tight-binding reference calculations if the damping factors are neglected, $g_U = 1$, as displayed in Fig. 1. If, however, the kernel factors g_U are taken into account, the important features of the density of states are removed, making it unsuitable for the prediction of structural stability. Therefore higher moments need to be taken into account before the expansion will sensibly converge to the tight-binding reference.

In order to avoid the loss of structure in the KPM for low-moments expansion, we combine it with the analytic BOP approximation of the continued fraction expansion discussed in Sec. III. In this way, the important low moments up to n_{\max} , which have been explicitly calculated, are only slightly damped such that the relevant structure of the density of states is maintained. This leads to a significantly improved convergence of the expansion as a function of n_{\max} . We illustrate our approach for an sp -valent TB model of Si.³⁷ For systems with band gaps, the simple approximation of a constant terminator, $a_n = a_{i\alpha}^{(\infty)}$ and $b_n = b_{i\alpha}^{(\infty)}$, is not suitable because the recursion coefficients oscillate as n approaches infinity. As a simple approximation, we assume for the present paper that the period of the oscillations along the recursion chain is two, which allows for one gap in the band,²⁷ and estimate the amplitude of the oscillation in the terminator from the average of the highest and third-highest recursion coefficients and from the average of the second-highest and fourth-highest recursion coefficients, respectively.

Figure 4 shows the density of states of silicon as calculated in TB and analytic BOP. The oscillation in the terminator leads

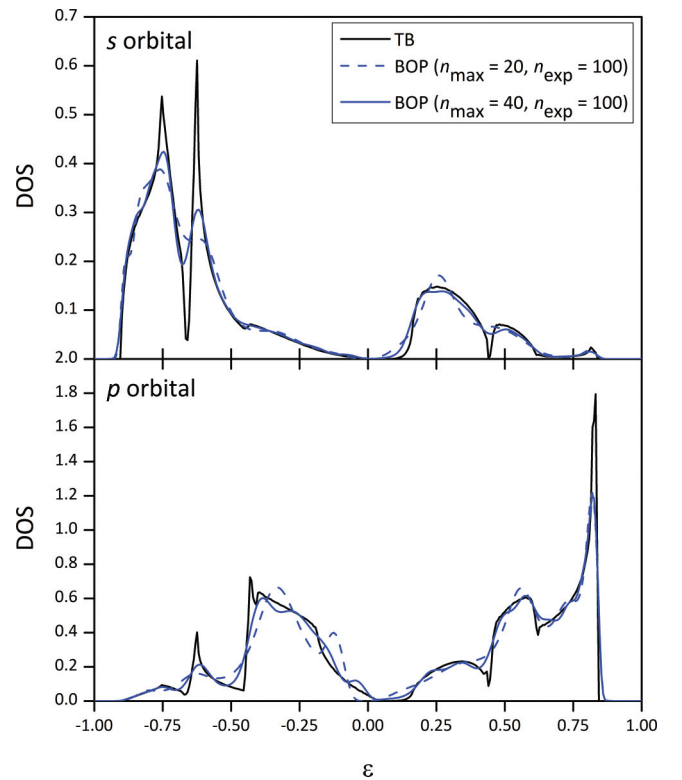


FIG. 4. (Color online) Comparison of the tight-binding density of states for Si with analytic BOP expansions of $n_{\max} = 20$ and 40 moments.

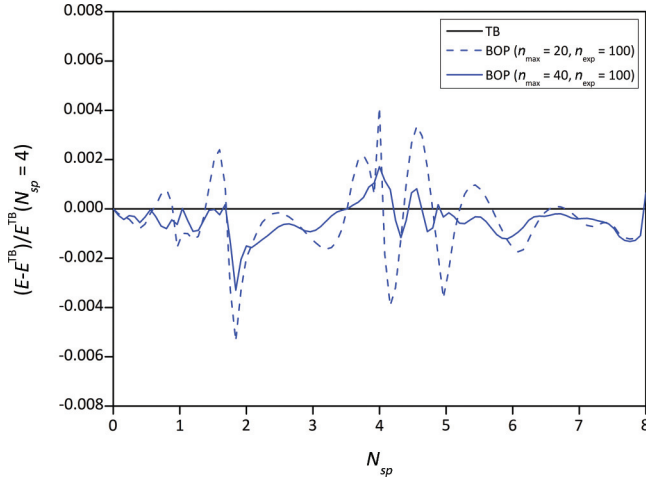


FIG. 5. (Color online) Convergence of the bond energy with respect to the TB reference bond energy for Si with $n_{\max} = 20$ and 40 moments analytic BOP expansions. The energy differences have been normalized by the TB bond energy at half-full band.

to a fair reproduction of the TB reference density of states including the band gap for the 20-moments approximation. At 40 moments, the analytic BOP density of states agrees very well with the tight-binding reference. The same holds for the energy differences. In Fig. 5, small deviations are observed for the 20-moments approximations, these differences have essentially disappeared at 40 moments.

V. CALCULATION OF FORCES

The expressions derived in Sec. IVC of Ref. 24 may be used to calculate the binding energy and to evaluate the forces on the atoms. To this end, the expansion coefficients $\sigma_{i\alpha}^{(n)}$ with $n = 1, \dots, n_{\exp}$ are obtained from the recursion coefficients $\{\hat{a}_k, \hat{b}_k\}$ following Eq. (A7), the recursion coefficients in turn are obtained from the moments $\mu_{i\alpha}^{(m)}$ with $m = 0, \dots, n_{\max}$. The derivatives of the Chebyshev moments with respect to a parameter Λ may then be related to the derivatives of the moments using the chain rule:

$$\frac{\partial \sigma_{i\alpha}^{(n)}}{\partial \Lambda} = \sum_{k=0}^{n_{\exp}/2} \sum_{l=0}^{n_{\max}/2} \sum_{m=0}^{n_{\max}} \left\{ \frac{\partial \sigma_{i\alpha}^{(n)}}{\partial \hat{a}_k} \left[\frac{\partial \hat{a}_k}{\partial a_l} \frac{\partial a_l}{\partial \mu_{i\alpha}^{(m)}} + \frac{\partial \hat{a}_k}{\partial b_l} \frac{\partial b_l}{\partial \mu_{i\alpha}^{(m)}} \right] + \frac{\partial \sigma_{i\alpha}^{(n)}}{\partial \hat{b}_k} \left[\frac{\partial \hat{b}_k}{\partial a_l} \frac{\partial a_l}{\partial \mu_{i\alpha}^{(m)}} + \frac{\partial \hat{b}_k}{\partial b_l} \frac{\partial b_l}{\partial \mu_{i\alpha}^{(m)}} \right] \right\} \frac{\partial \mu_{i\alpha}^{(m)}}{\partial \Lambda}. \quad (41)$$

By inserting this derivative into the equations given in Ref. 24, the forces are readily obtained. The calculation of the forces is exact also for values of $a_{i\alpha}^{(\infty)}$ and $b_{i\alpha}^{(\infty)}$ that vary locally from one atom and orbital to the other. This is an advantage over other moments or recursion-based methods^{9,38} that assume identical values of $a_{i\alpha}^{(\infty)}$ and $b_{i\alpha}^{(\infty)}$ for all atoms and orbitals in order to be able to calculate the forces from straightforward derivatives of the global moments $\mu^{(n)} = \sum_{i\alpha} \mu_{i\alpha}^{(n)}$ and therefore implicitly require an expression for the energy that must be linear with $\mu_{i\alpha}^{(n)}$.

VI. CONCLUSION

By approximating higher moments of the density of states from straightforward terminations of the recursion chain, the analytic bond-order potentials efficiently approximate the continued fraction expansion. In contrast to the continued fraction expansion, the analytic BOP density of states may be integrated analytically and the exact forces for a locally varying bandwidth may be obtained. For systems with band gaps, the application of the kernel damping factors in the analytic BOPs, in analogy to the KPM, efficiently removes oscillations in the density of states. This enables the application of the analytic BOPs to open systems and, together with the inclusion of charge transfer and magnetism,²⁴ this will allow the modeling of phase transformations from close-packed to open phases and vice versa.

ACKNOWLEDGMENTS

We acknowledge financial support through ThyssenKrupp AG, Bayer MaterialScience AG, Salzgitter Mannesmann Forschung GmbH, Robert Bosch GmbH, Benteler Stahl/Rohr GmbH, Bayer Technology Services GmbH, and the state of North-Rhine Westphalia as well as the European Commission in the framework of the ERDF.

APPENDIX A: RECURSIVE CALCULATION OF MOMENTS

If one defines $\xi_k^{(n)}$ as the interference path that starts on orbital u_0 and ends on orbital u_k ,

$$\xi_k^{(n)} = \langle u_k | \hat{H}^n | u_0 \rangle, \quad (A1)$$

then the moments are obtained from the self-returning hopping paths as

$$\mu_{i\alpha}^{(n)} = \xi_0^{(n)} = \langle u_0 | \hat{H}^n | u_0 \rangle. \quad (A2)$$

Because of the tridiagonal form of the recursion chain Hamiltonian, the matrix elements with $k > n$ all vanish, $\xi_k^{(n)} = 0$ and the moment may also be obtained from products of the interference paths:

$$\mu_{i\alpha}^{(n)} = \sum_k \xi_k^{(m)} \xi_k^{(n-m)}, \quad (A3)$$

where $n \geq m \geq 0$. From this expression, the derivative of the moments with respect to the chain Hamiltonian may be obtained simply by taking into account that all interference paths that depend on a_k or b_k must also pass through the k^{th} state $|u_k\rangle$ of the recursion chain,

$$\frac{\partial \mu_{i\alpha}^{(n)}}{\partial a_k} = \sum_{m=k}^{n-m-1} \xi_k^{(m)} \xi_k^{(n-m-1)}, \quad (A4)$$

$$\frac{\partial \mu_{i\alpha}^{(n)}}{\partial b_k} = 2 \sum_{m=k}^{n-m-1} \xi_k^{(m)} \xi_{k+1}^{(n-m-1)}. \quad (A5)$$

Similar relations exist for the evaluation of the Chebyshev moments $\langle u_0 | U_n(\hat{h}) | u_0 \rangle$. We define

$$\zeta_k^{(n)} = \langle u_k | U_n(\hat{h}) | u_0 \rangle, \quad (A6)$$

such that $\sigma_{i\alpha}^{(n)} = \zeta_0^{(n)}$. Using the recursion relation of the Chebyshev polynomials of the second kind, $U_{n+1}(\epsilon) = 2\epsilon U_n(\epsilon) - U_{n-1}(\epsilon)$ (with $U_0 = 1$ and $U_{-1} = 0$), a recursive calculation of $\zeta_k^{(n+1)}$ may be achieved from

$$\zeta_k^{(n+1)} = 2[\hat{a}_k \zeta_k^{(n)} + \hat{b}_k \zeta_{k-1}^{(n)} + \hat{b}_{k+1} \zeta_{k+1}^{(n)}] - \zeta_k^{(n-1)}, \quad (\text{A7})$$

with $\hat{a}_k = \frac{a_k - a_{i\alpha}^{(\infty)}}{2b_{i\alpha}^{(\infty)}}$ and $\hat{b}_k = \frac{b_k}{2b_{i\alpha}^{(\infty)}}$. Starting from $n = 0$, for a given value of n , this is iterated for $k = 0 \dots n$ (or $k = 0 \dots n_{\text{rec}}$ if $n > n_{\text{rec}} = n_{\text{max}}/2$) and, subsequently, repeated for n up to n_{max} .

APPENDIX B: CHOICE OF TERMINATOR COEFFICIENTS

We estimate the bottom and the top of the band for each orbital using Gerschgorin's circle theorem.³⁵ The eigenvalues of an $n \times n$ matrix with, in general, complex matrix elements

a_{ij} are contained in discs centered on the diagonal matrix elements a_{ii} with diameter $r_i = \sum_j |a_{ij}|$. For the tridiagonal recursion matrix, this means that all the eigenvalues are contained in the interval

$$E_{\text{bottom}} = \text{Min}\{a_n - b_n - b_{n+1}\}, \quad (\text{B1})$$

$$E_{\text{top}} = \text{Max}\{a_n + b_n + b_{n+1}\}, \quad (\text{B2})$$

where Min and Max refers to the minimum and maximum values, respectively, for $n = 0, \dots, n_{\text{rec}} - 1$. By choosing

$$a_{i\alpha}^{(\infty)} = (E_{\text{top}} + E_{\text{bottom}})/2, \quad (\text{B3})$$

$$b_{i\alpha}^{(\infty)} = (E_{\text{top}} - E_{\text{bottom}})/4, \quad (\text{B4})$$

we ensure that the complete spectrum is contained in the interval E_{bottom} to E_{top} and therefore the kernel (40) guarantees a strictly positive density of states.

¹F. Cyrot-Lackmann, *Adv. Phys.* **16**, 393 (1967).

²F. Ducastelle and F. Cyrot-Lackmann, *J. Phys. Chem. Solids* **31**, 1295 (1970).

³F. Ducastelle and F. Cyrot-Lackmann, *J. Phys. Chem. Solids* **32**, 285 (1971).

⁴D. G. Pettifor and M. Aoki, *Phil. Trans. R. Soc. A* **334**, 439 (1991).

⁵D. G. Pettifor, *Bonding and Structure in Molecules and Solids* (Oxford University Press, Oxford, 1995).

⁶B. Seiser, T. Hammerschmidt, A. N. Kolmogorov, R. Drautz, and D. G. Pettifor, *Phys. Rev. B* **83**, 224116 (2011).

⁷M. Nastar and F. Willaime, *Phys. Rev. B* **51**, 6896 (1995).

⁸D. R. Bowler, M. Aoki, C. M. Goringe, A. P. Horsfield, and D. G. Pettifor, *Modelling Simul. Mater. Sci. Eng.* **5**, 199 (1997).

⁹S. Goedecker, *Rev. Mod. Phys.* **71**, 1085 (1999).

¹⁰D. R. Bowler and T. Miyazaki, *Rep. Prog. Phys.* **75**, 036503 (2012).

¹¹R. Haydock, *Solid State Phys.* **35**, 216 (1980).

¹²P. E. A. Turchi and F. Ducastelle, in *The Recursion Method and its Applications*, Springer Series in Solid State Sciences, edited by D. G. Pettifor and D. L. Weaire, Vol. 58 (Springer, Berlin, 1985), p. 104.

¹³D. G. Pettifor, *Phys. Rev. Lett.* **63**, 2480 (1989).

¹⁴M. Aoki and D. G. Pettifor, *Int. J. Mod. Phys. B* **7**, 299 (1993).

¹⁵M. Aoki, *Phys. Rev. Lett.* **71**, 3842 (1993).

¹⁶A. P. Horsfield, A. M. Bratkovsky, M. Fearn, D. G. Pettifor, and M. Aoki, *Phys. Rev. B* **53**, 12694 (1996).

¹⁷R. N. Silver, H. Röder, A. F. Voter, and J. D. Kress, *J. Comp. Phys.* **124**, 115 (1996).

¹⁸A. F. Voter, J. D. Kress, and R. N. Silver, *Phys. Rev. B* **53**, 12733 (1996).

¹⁹S. Goedecker and L. Colombo, *Phys. Rev. Lett.* **73**, 122 (1994).

²⁰S. Goedecker and M. Teter, *Phys. Rev. B* **51**, 9455 (1995).

²¹A. Weiße, G. Wellein, A. Alvermann, and H. Fehske, *Rev. Mod. Phys.* **78**, 275 (2006).

²²M. W. Finnis and J. E. Sinclair, *Philos. Mag. A* **50**, 45 (1984).

²³R. Drautz and D. G. Pettifor, *Phys. Rev. B* **74**, 174117 (2006).

²⁴R. Drautz and D. G. Pettifor, *Phys. Rev. B* **84**, 214114 (2011).

²⁵C. Lanczos, *J. Res. Natl. Bur. Stand.* **45**, 225 (1950).

²⁶A. Horsfield, *Mater. Sci. Eng. B* **37**, 219 (1996).

²⁷P. Turchi, F. Ducastelle, and G. Treglia, *J. Phys. C: Solid State Phys.* **15**, 2891 (1982).

²⁸R. Haydock and C. M. M. Nex, *Phys. Rev. B* **74**, 205121 (2006).

²⁹R. Haydock and C. M. M. Nex, *Phys. Rev. B* **82**, 205114 (2010).

³⁰D. G. Pettifor, *J. Phys. F* **7**, 613 (1977).

³¹O. K. Andersen, W. Klose, and H. Nohl, *Phys. Rev. B* **17**, 1209 (1978).

³²R. N. Silver and H. Röder, *Phys. Rev. E* **56**, 4822 (1997).

³³K. Bandyopadhyay, A. K. Bhattacharya, P. Biswas, and D. A. Drabold, *Phys. Rev. E* **71**, 057701 (2005).

³⁴A. Weiße and H. Fehske, *Lect. Notes Phys.* **739**, 545 (2008).

³⁵S. Gerschgorin, *Bulletin de l'Académie des Sciences de l'URSS* **6**, 749 (1931).

³⁶R. Andreani and D. K. Dimitrov, *Rocky Mountain J. Math.* **33**, 759 (2003).

³⁷J. Gehrmann, A. N. Kolmogorov, R. Drautz, and D. G. Pettifor (unpublished).

³⁸A. P. Horsfield, *Phil. Mag.* **89**, 3287 (2009).